Available online at www.sciencedirect.com
SCIENCE DIRECT®
C. R. Mecanique 331 (2003) 189–196
COMPTES RENDUS MECANIQUE

Analysis of random nonlinear water waves: the Stokes–Woodward technique

La technique de Stokes–Woodward pour l'analyse de vagues aléatoires non linéaires

Tanos Elfouhaily [a], Maminirina Joelson [a], Stéphan Guignard [a], Hubert Branger [a], Donald R. Thompson [b], Bertrand Chapron [c], Douglas Vandemark [d]

[a] *Centre national de la recherche scientifique (CNRS), institut de recherche sur les phénomènes hors equilibre (IRPHE), Marseille, France*
[b] *The Johns Hopkins University, Applied Physics Laboratory, 11100 Johns Hopkins Road, Laurel, MD 20723-6099, USA*
[c] *Département d'océanographie spatiale, IFREMER, centre de Brest, BP 70, 29280 Plouzané, France*
[d] *NASA Goddard Space Flight Center, Laboratory for Hydrospheric Processes, Wallops Island, VA 23337, USA*

Received 14 October 2002; accepted after revision 24 February 2003

Presented by Paul Clavin

Abstract

A generalization of the Woodward's theorem is applied to the case of random signals jointly modulated in amplitude and frequency. This yields the signal spectrum and a rather robust estimate of the bispectrum. Furthermore, higher order statistics that quantify the amount of energy in the signal due to nonlinearities, e.g., wave–wave interaction in the case of water waves, can be inferred. Considering laboratory wind generated water waves, comparisons between the presented generalization and more standard techniques allow to extract the spectral energy due to nonlinear wave–wave interactions. It is shown that our analysis extends the domain of standard spectral estimation techniques from narrow-band to broad-band processes. ***To cite this article: T. Elfouhaily et al., C. R. Mecanique 331 (2003).***

Résumé

Une généralisation du théorème de Woodward est appliquée au cas d'un signal aléatoire modulé en amplitude et en fréquence. Le spectre du signal ainsi qu'une estimation robuste du bispectre sont obtenues grace à cette nouvelle technique. En sus, des moments statistiques d'ordre supérieur quantifiant l'énergie due aux non linéarités, i.e., aux interactions entre vagues dans le cas des ondes de surface, sont évalués. L'énergie spectrale d'interaction non linéaire est extraite grâce à la comparaison de la présente méthode, à des méthodes plus classiques lors de l'analyse de signaux de vagues de vent fort générées en soufflerie. Il est finalement montré que notre technique étend le domaine des méthodes d'estimation spectrale aux processus large bande. ***Pour citer cet article : T. Elfouhaily et al., C. R. Mecanique 331 (2003).***

E-mail addresses: elfouhaily@irphe.univ-mrs.fr (T. Elfouhaily), guignard@irphe.univ-mrs.fr (S. Guignard), branger@irphe.univ-mrs.fr (H. Branger), donald.r.thompson@jhuapl.edu (D.R. Thompson), Bertrand.Chapron@ifremer.fr (B. Chapron), vandemark@gsfc.nasa.gov (D. Vandemark).

1631-0721/03/$ – see front matter
doi:10.1016/S1631-0721(03)00055-X

Keywords: Fluid mechanics; Mode coupling; Wave–wave interaction; Horizontal asymmetry; Vertical asymmetry; Bispectrum; Amplitude modulation; Frequency modulation

Mots-clés : Mécaniques des fluides ; Couplage de mode ; Interaction vague–vague ; Dissymétrie verticale ; Dissymétrie horisontale ; Bispectre ; Modulation d'amplitude ; Modulation de fréquence

Version française abrégée

La complexité des vagues de vent a amené de nombreux auteurs à les modéliser par une superposition d'ondes aléatoires d'amplitudes et de fréquences fortement modulées. Lors de la simulation d'ondes de surface non linéaires, Elfouhaily et al. [2] ont montré qu'il était nécessaire d'injecter en entrée de la simulation, un spectre débarrassé des interactions non linéaires, sous peine de voir le spectre de sortie différer considérablement du spectre réel. Afin d'obtenir ce spectre dit « spectre nu » d'un signal réel large bande, nous avons développé une généralisation du théorème de Woodward [11] pour un signal aléatoire modulé en fréquence mais aussi en amplitude. Ainsi, un tel signal a un spectre de la forme (2). Pour évaluer le spectre de ce signal, il faut évaluer la probabilité conjointe de quatre variables aléatoires. Afin de simplifier le problème nous avons exprimé cette généralisation sous deux formes : dans le cas d'indices de modulation infinis de l'amplitude et de la fréquence, nous obtenons comme limite de (2), la forme (3), qui est le spectre d'un signal dont l'amplitude, la fréquence et la phase sont aléatoires mais indépendantes du temps. C'est donc le « spectre nu » où les échanges d'énergie entre ses différentes composantes spectrales du signal n'ont pas lieu. Dans un deuxième temps, l'amplitude et la phase du signal sont toujours supposées aléatoires mais elles comprennent une dépendance explicite en temps (5). Un développement de Stokes du signal est ainsi obtenu (7) et son spectre s'exprime (9) sous la forme du spectre nu augmenté de deux intégrales comprenant les probabilités conjointes des dissymétries et de la fréquence instantannée. L'évaluation de ce spectre dit « spectre habillé » ne nécessite plus que trois histogrammes bidimensionnels, ceux de l'amplitude et des dissymétries horizontales et verticales en fonction de la fréquence. De même l'équation (10) montre qu'il suffit d'évaluer deux histogrammes tridimensionnels pour évaluer le bispectre. Enfin, les histogrammes précédemment cités sont estimés à partir du signal de hauteur d'eau dans une soufflerie en présence de vagues de vent. Les valeurs de la féquence instantannée sont évaluées par la méthode de zero-crossing [17]. Pour une période donnée, les valeurs de a, α, β sont calculées comme illustré Fig. 3. La Fig. 4 présente le spectre du signal réel (courbe tremblante), le spectre nu (continu, bas), le spectre de Woodward (continu, haut), le spectre habillé (tirés-points), le spectre habillé diminué de l'intégrale sur la dissymétrie horisontale (tirés). Le spectre de Woodward sur-estime l'énergie aux fréquences supérieures au pic, car par hypothèse, l'amplitude (constante) ne dépend pas de la fréquence, alors que l'énergie des hautes fréquences du champ réel est plus faible. Le spectre nu sous-estime l'énergie à ces mêmes fréquences car les interactions non linéaires sont absentes. Enfin le « spectre habillé » reproduit fidèlement le spectre obtenu par transformée de Fourrier. De même pour le bispectre, la Fig. 5 montre le bon accord entre le « bispectre habillé » et le bispectre mesuré (section unidimentionnelle de la transformée de Fourrier bidimentionnelle de la fonction d'autocorrelation de troisième ordre 10). Cela démontre la capacité de la méthode de Stokes–Woodward à différencier le spectre nu du spectre habillé et met en évidence l'étroite corrélation entre les caractéristiques géométriques de la surface libre (dissymétries) et les effets non linéaires de couplage de modes.

1. Introduction and issues

According to common observations, a recent study [1] has demonstrated that wind waves cannot be characterized by a deterministic system dynamically affected by nonlinearities.This leads to a description of water waves as a superposition of random waves characterized by highly irregular amplitudes and frequencies.

When simulating nonlinear water waves, [2] demonstrated that a common inconsistency was to use an empirically determined spectrum as input, despite the fact that, due to the short wave energy increase by wave–wave

interaction, the output spectrum will deviate considerably from the measurements. Examples of such misuse have already been identified in [2,3] which are concerned with understanding the electromagnetic bias observed by radar altimeters over the ocean surface. The contribution by [2] suggests the need for an input spectrum, termed the "bare" spectrum, devoid of any nonlinear interaction. The output spectrum is then obtained from nonlinear interactions of all the modes present at the input to form the so-called "dressed" spectrum. Unfortunately, the "bare" spectrum does not itself yield easily to measurement since nonlinear wave–wave interactions cannot be turned off during the measurement of the surface wave spectrum. Higher order hydrodynamic interactions [4] will distort the input spectrum even further hampering the study of its effect on, among other things, several remote sensing parameters [5].

In the narrow-banded spectrum case, according to [6–9], the weak modulations that characterises surface waves are time independent or slowly varying random variables. However, this narrow-band formulation is insufficient to explain the complexity of water waves when higher-order statistics must be included due to the asymmetric behavior caused by nonlinear wave–wave interactions. In this case, large deviations from a narrow-band approximation can be observed especially under conditions of wind generated waves, and the random variables are no longer time independent [10]. Under these conditions, the processes become broad band in nature.

Woodward's theorem [11] shows that a frequency or phase modulated signal has a spectrum expressed by $S(f) \approx \frac{A^2}{2} P_{\dot{\phi}}(f - f_c)$, $P_{\dot{\phi}}$ being the probability density function of the modulating instantaneous frequency, A a constant amplitude, f_c the central or carrier frequency. For simplicity negative frequencies have been folded onto positive frequencies since the signal under study is real.

In this study, we model random nonlinear surface waves as broad-band processes with the objective of properly characterizing the spectral content of these signals. A distinction will be made between spectral density due to nonlinearity as opposed to that when no wave–wave interactions are present. To achieve these goals, we generalize Woodward's theorem [11] to include amplitude modulations under moderately large indices of modulations: in this context, the form of the signal to be studied is then

$$\eta(t) = a\left(\frac{t}{\mu}\right) \cos\left[\omega_c t + 2\pi \int_0^t D\left(\frac{\tau}{\nu}\right) \mathrm{d}\tau\right] \tag{1}$$

where $a(t/\mu)$ is a random process with an index of modulation μ and $D(\tau/\nu)$ is the modulating random instantaneous frequency with index ν. As suggested by [12], assuming large enough modulation indices μ and ν, statistical stationnarity for a and D, and following [13], we obtain the corresponding spectrum (where $\omega = 2\pi f$):

$$S(f) \approx \frac{1}{2} \int \left[a^2 - \frac{\dot{a}^2}{4\mu^2}\left(\frac{\partial^2}{\partial \omega^2}\right)\right] P\left(a, \dot{a}, \omega - \frac{\dot{\omega} t}{\nu}, \dot{\omega}\right) \mathrm{d}a\, \mathrm{d}\dot{a}\, \mathrm{d}\dot{\omega} \tag{2}$$

This generalization of Woodward's theorem requires knowledge of the joint distribution of four random processes as opposed to that of one process in the original theorem. This generalization to a four dimensional distribution in (2) is generally not useful since it is impractical to estimate such multidimensional distributions from the time series of the signal itself. We shall now present in the following section, a more practical formulation of this generalization where a joint distribution with fewer dimensions is required. We will then compare our development with experimental data obtained from a wind-wave tank, where a clear difference between the bare and the dressed spectra is shown.

2. The Stokes–Woodward technique

2.1. Statistical modulation

As mentioned above, a brute force generalization of Woodward's theorem as in (2) is inefficient and may even be unstable if the time series under study is not long or stationary enough. It is easy to notice that (2) reaches a very

practical limit if both indices of amplitude and frequency modulations, μ and ν respectively, are nearly infinite. In this limit, (2) reduces to what we call the bare spectrum

$$S_{\text{bare}}(f) \approx \frac{1}{2}\int a^2 P(a, f)\,\mathrm{d}a \tag{3}$$

This approximation is very practical and requires only the estimation of a two-dimensional histogram. However, this practicality is gained at the expense of neglecting the temporal modulations of the amplitude and frequency within the scale of the dominant time period. In other words, the slow modulations are modeled by random processes that vary from one period to the next. More simply, the high index approximation in (3) is actually an exact formulation for a random process of this form

$$\eta(t) = a\cos(\omega t + \theta) \tag{4}$$

where a, ω, and θ are three time-independent random variables. The amplitude a and the pulsation $\omega = 2\pi f$ can be statistically dependent, while θ is a uniformly distributed phase and independent of these other variables. This requirement on the uniformity of the phase guarantees that the signal is stationary and therefore that the autocorrelation and the spectral functions are univariate. The "bare" subscript in (3) refers to the fact that the process in (4) has lost all nonlinearity or phase coupling of harmonics.

2.2. Temporal and statistical modulation

The high index limit in (3) is very illustrative and permits the reformulation of our newly generalized theorem into a simpler form. The time modulation present in (1) can now be replaced by a random modulation as in (4). Let us reformulate the modulation as

$$\eta(t) = \big[a + \Delta a(t)\big]\cos\big[\omega t + \Delta\phi(t) + \theta\big] \tag{5}$$

where the time dependence is explicitly shown in addition to the implicit random dependence of all the parameters except the time variable. The key representation of our simplified expression is in the time dependence of the modulation that can be expanded in Fourier series about the random frequency ω as

$$\Delta a(t) = \alpha_c\cos(\omega t + \theta) + \alpha_s\sin(\omega t + \theta) + \cdots \tag{6a}$$

$$\Delta\phi(t) = \beta_c\cos(\omega t + \theta) + \beta_s\sin(\omega t + \theta) + \cdots \tag{6b}$$

The signal in (5) can be further expanded keeping only terms of linear order in the parameters α_c, α_s, β_c, and β_s to find a more poignant form given by

$$\eta(t) = \lambda + a\cos[\omega t + \theta] + \alpha\cos\big[2(\omega t + \theta)\big] + \beta\sin\big[2(\omega t + \theta)\big] + \cdots \tag{7}$$

where the coefficients α and β of the second harmonic terms in (7) are related to the coefficients in (6) by

$$\lambda = \frac{a\beta_s + \alpha_s}{2}, \qquad \alpha = \frac{a\beta_s + \alpha_c}{2}, \qquad \beta = \frac{\alpha_s - a\beta_c}{2} \tag{8}$$

We remind the reader that all parameters in (7) are random variables except the time variable. Finally, not included in our analysis is the constant term λ. We save discussions of the significance of this term for a future publication. There is no influence of the presence or the absence of the constant term in the dataset selected for illustration in the current paper.

Eq. (7) represents a generalization to the Stokes wave in two regards. First, all parameters are random as opposed to the Stokes wave where all parameters must stay constant. Second, the sin( ) term generates asymmetries in the profile that are not included in a standard Stokes waveform. Its resemblance with the Stokes wave, however, did influence our choice for naming our analysis method, which uses Woodward's theorem and Stokes-like waveforms, the "Stokes–Woodward" technique. The random variables α and β explain the asymmetries of the waveform with

respect to a horizontal and vertical axes, respectively. These asymmetries appear in a random manner on the scale of the period of the wave as depicted by the random amplitude a and random frequency ω.

Similar to Eq. (4), the random Stokes-like waveforms in (7) yields a spectrum of the Woodward type but in a more accessible form than in (2). This form is given by

$$S_{\text{dressed}}(f) \approx S_{\text{bare}}(f) + \frac{1}{2}\int \alpha^2 P\left(\alpha, \frac{f}{2}\right) \mathrm{d}\alpha + \frac{1}{2}\int \beta^2 P\left(\beta, \frac{f}{2}\right) \mathrm{d}\beta \tag{9}$$

In this final form, two single integrals are needed in addition to the single integration over the amplitude already present in the "bare" spectrum of (3). We associate the spectrum in (9) with the "dressed" spectrum discussed in the introduction, and interpret the terms added to the bare spectrum as contributing to the energy increase at higher frequencies due to the nonlinearities or mode coupling. This energy augmentation therefore provides the difference between the bare and the dressed spectra as discussed in [2]. The difference can also be assimilated with the bicoherence function of phase coupling as introduced by [14] and utilized by [15]. Indeed, energy of phase coupling to second order is another manifestation of the bispectrum defined as the Fourier transform of the skewness function using a third order cumulant. The bispectrum is defined as the 2D Fourier transform of the bivariate skewness function $R(\tau_1, \tau_2) = \langle \eta(t)\eta(t+\tau_1)\eta(t+\tau_2)\rangle$. The description of the vertical and horizontal asymmetries of the waveform opens the way for the definition of a very robust bispectral estimate derived from our Stokes–Woodward technique. The bispectrum takes the form

$$B(f) = B\left(f, \frac{f}{2}\right) \approx \frac{1}{4}\iint \alpha a^2 P\left(\alpha, a, \frac{f}{2}\right) \mathrm{d}\alpha \mathrm{d}a + \mathrm{i}\frac{1}{4}\iint \beta a^2 P\left(\beta, a, \frac{f}{2}\right) \mathrm{d}\beta \, \mathrm{d}a \tag{10}$$

where now two three-dimensional histograms are needed in order to evaluate the double integration over the amplitude and the asymmetries. It is no surprise that the height (or vertical) asymmetry α yield the real part of the bispectrum while the horizontal asymmetry β yield the imaginary part. We shall show in the next section that the estimation of the "bare" and "dressed" spectra as well as the bispectrum is very robust and can lead to interesting interpretations of the surface wave physics.

3. Comparison with data

3.1. Experimental data

The Stokes–Woodward technique is now tested using a time series generated by measuring the height of the water surface at a fixed point in a wind-wave tank. The signals were obtained from the Ocean-Atmosphere Interaction facility in Marseille with a capacitance wave gauge. The pool dimensions in the tank are $40 \times 3 \times 1$ meters for the length, width, and depth, respectively. The air tunnel's ceiling is 1.5 m above the water surface. For a detailed description of the flume-tank, the reader is referred to [16]. In order to generate highly nonlinear waves where mode coupling should be significant, we chose to sample wind-generated waves under high wind conditions with wind speeds higher than 10 m/s with a fetch of 25 m but without paddle waves. Long time series were acquired at high frequency sampling. Duration and sampling rate were of the order of 30 minutes and 100 Hz, respectively. Fig. 1 shows a short sample of the time series of surface elevations. High modulations and group occurrences are easily visible in this short segment. In order to estimate the instantaneous amplitude a, frequency f, vertical asymmetry α and horisontal asymmetry β in (7), we implemented the zero-crossing algorithm as explained in [17]. Ambiguities related to the definition of the instantaneous frequency [18] are not dealt with here, but will be left for later contributions when more exact algorithms will be used. We mention that the zero-crossing algorithm is well defined as long as the broad-band signal has a unimodal spectrum with no low frequency components or high noise contaminations. Practical estimators for the four random variables, a, $\omega = 2\pi/T$, α, and β are taken as Fig. 3 illustrates.

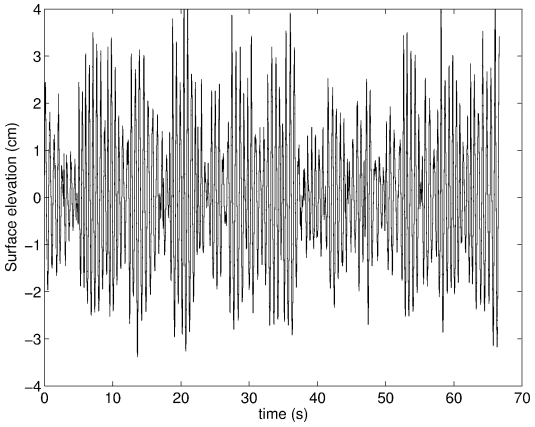

Fig. 1. Time series of the surface elevation. Modulations appears clearly.

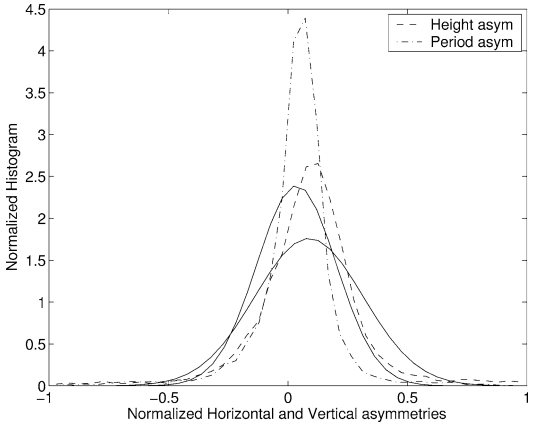

Fig. 2. Normalized horizontal (dashed–dotted) and vertical (dashed) asymmetries.

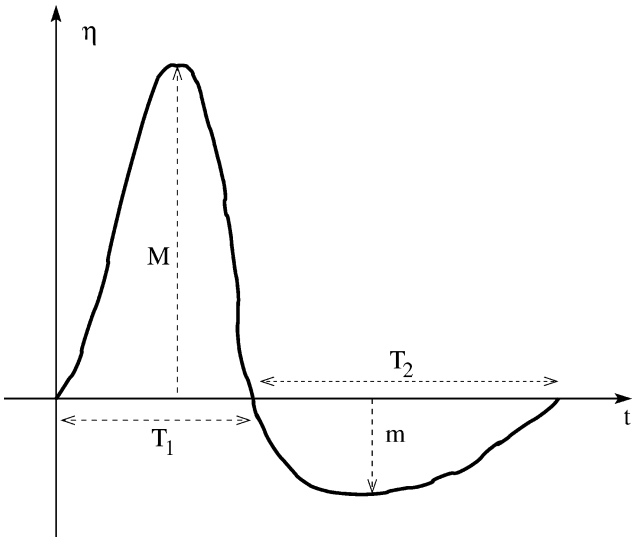

Fig. 3. Sketch plot to show the definitions of the paratemeters (M, m, T_1, T_2) used to estimate the instantaneous amplitude $a = (M - m)/2$, period $T = T_1 + T_2$, vertical $\alpha = (M + m)/2$ and horizontal $\beta = a\pi(T_1 - T_2)/(T_1 + T_2)/2$ asymmetries.

3.2. Analysis results

Fig. 2 illustrates the stability of the estimators for the asymmetry parameters as shown in terms of their normalized histograms.

The vertical asymmetry (dashed line) α is normalized by the amplitude a where the horizontal asymmetry (dased dotted line) β is normalized by $a\frac{\pi}{2}$. A striking difference is easily noticeable between these histograms and the Gaussian distributions shown for reference by the solid lines in the figure. Indeed, the histograms seem to be highly peaked with some skewness. The kurtosis is very high and on the order of 4 and 6 for the vertical (α) and horisontal (β) asymmetries, respectively. The ragged line in Fig. 4 shows the Fourier spectrum of the time series. Using a standard spectrum such as this, one is not able to differentiate between energies coming from linear or nonlinear waves.

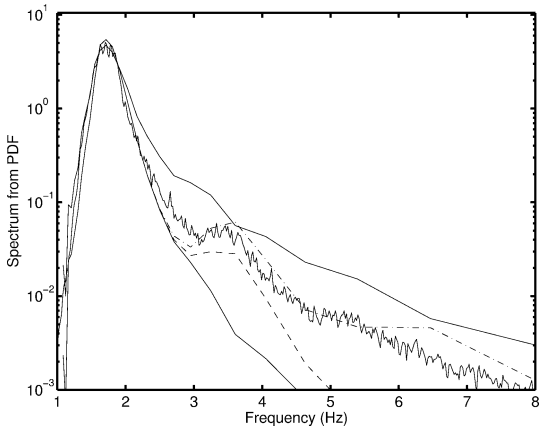

Fig. 4. Fourier spectrum of the experimental wave profile (ragged line). Woodward spectrum (upper solid curve). "Bare" spectrum (lower solid line). "Bare" augmented by the vertical asymmetry (dashed curve). "Dressed" spectrum (dashed–dotted curve).

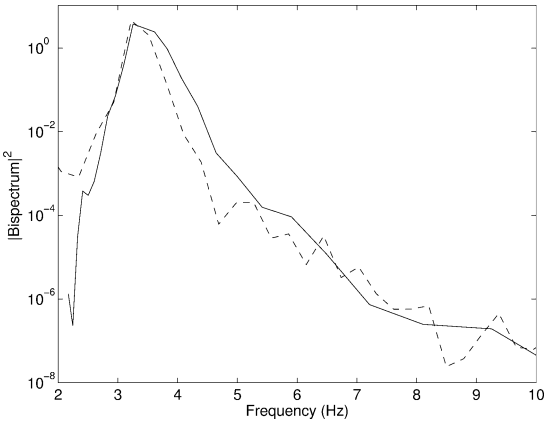

Fig. 5. Comparison of bispectra's modulus square. "Dressed" bispectra (solid curve). Fourrier transform of the skewness function (dashed curve). Plots normalized by their corresponding total integral.

The Woodward spectrum as defined in Section 1, is the highest solid curve in Fig. 4. One can see that this curve over-estimates the measured spectrum because of the underlying Woodward assumption that, on the contrary to the real signal, the amplitude is not modulated, and that only frequency modulation is present. The over-estimation of the spectral tail is therefore due to the fact that the real amplitude is modulated and also correlated with the frequency in such a manner that high frequency waves have less energy. The lowest solid line in Fig. 4 is the "bare" spectrum as defined by (3) where both amplitude and frequency modulations are accounted for with no asymmetries or phase coupling. It is instructive to notice that the "bare" spectrum underestimates the energy in the tail of the measured spectrum. This under estimation is due to the implicit assumption in (3) that the indices of modulations are very high and therefore any nonlinearity caused by time-dependent modulations is neglected. The "dressed" spectrum (9) is shown in Fig. 4 by the dashed–dotted curve. This curve accounts for most of the energy present in the measured Fourier spectrum. Both vertical and horizontal asymmetries contribute to the energy at high frequencies. This can be seen by the fact that the dashed curve shown in Fig. 4, which includes modulation of only the height (α) asymmetry, under estimates the high-energy content of the measured spectrum. It therefore seems apparent that our Stokes–Woodward technique explains the energy due to mode coupling. A direct measure of the coupling can also be achieved by calculating the bispectrum as defined in (10). The result of this computation is shown in Fig. 5 in terms of its modulus square. The high stability of the bispectral estimate up to a quite high frequency demonstrates the wide domain of applicability of our technique. The peak present in the bispectrum indicates that many frequencies or harmonics are coupled with their fundamental counterparts at lower frequencies. It is therefore important to treat the ensemble of frequencies as two correlated random sets. Based on the results of the comparisons presented in this section, we believe our technique can accurately interpret the occurrences of instantaneous amplitudes, frequencies, vertical and horizontal asymmetries. This demonstrates the capability to detecting mode coupling in spectral domain of second statistical order without performing bispectral analysis.

4. Conclusion

A generalization of Woodward's theorem is successfully obtained by including random amplitude modulations in addition to frequency modulations. The original theorem stated that a good approximation of the energy spectrum of a frequency modulated signal is the probability density function of the instantaneous frequencies when the index

of modulation is high. Our generalization starts by including the random amplitude modulation which yield a simple spectrum expressed as a single integral over the instantaneous amplitudes and the joint distribution of amplitude and frequency as shown in (3). It is noted that this spectrum is devoid of any nonlinearity or mode coupling because over the scale of a characteristic period, the wave is considered as simply harmonic (a sine wave). Asymmetries in the wave profile must be introduced in order to capture residual energy not explained by the "bare" spectrum. To account for this residual energy, we have proposed a second generalization of Woodward's theorem that utilizes a Stokes-like waveform in which all the parameters are random except the time variable. Our procedure is termed the Stokes–Woodward technique since it combines a generalization of Woodward's theorem with a Stokes-like random wave profile.

The second generalization provides a practical formulation for the "dressed" spectrum where nonlinearities up to the second order are included (9). This second order coupling between modes initiates the existence of the bispectrum which can be formulated as in (10). It is demonstrated that when the Stokes–Woodward technique is applied to a time series of water-wave surface elevations, it discriminates between the "bare" and "dressed" spectrum, and also provides a robust estimate of the bispectrum. We recommend that the bare spectrum be used at the input of nonlinear system simulators as originally cautioned in [2].

Applications of the Stokes–Woodward technique will have great benefit in the analysis of nonlinear random processes present in several science fields. For example, it can readily be applied to remote sensing signals as already demonstrated by [19] even with the original formulation of Woodward's theorem.

References

[1] M. Joelson, A. Ramamonjiarisoa, A nonlinear second-order stochastic model of ocean surface waves, Oceanologica Acta 24 (5) (2001) 1–7.
[2] T. Elfouhaily, D.R. Thompson, B. Chapron, D. Vandemark, Weakly nonlinear theory and sea state bias estimations, J. Geophys. Res. 104 (C4) (1999) 7641–7647.
[3] T. Elfouhaily, D.R. Thompson, B. Chapron, D. Vandemark, Improved electromagnetic bias theory, J. Geophys. Res. 105 (C1) (2000) 1299–1310.
[4] T. Elfouhaily, D.R. Thompson, B. Chapron, D. Vandemark, Higher-order hydrodynamic modulation: theory and applications for ocean waves, Proc. Roy. Soc. London Ser. A 457 (2015) (2001) 2585–2608.
[5] T. Elfouhaily, D.R. Thompson, B. Chapron, D. Vandemark, Improved electromagnetic bias theory: Inclusion of hydrodynamic modulations, J. Geophys. Res. 106 (C3) (2001) 4655–4664.
[6] S. Bochner, Harmonic Analysis and the Theory of Probability, University California Press, California, USA, 1960.
[7] B. Kinsman, Wind Waves: Their Generation and Propagation in Ocean Surface, Prentice-Hall, Englewood Cliffs, NJ, USA, 1965.
[8] M.S. Longuet-Higgins, On the joint distribution of wave periods and amplitudes in random wave field, Proc. Roy. Soc. London Ser. A 389 (1983) 241–258.
[9] M.A. Tayfun, On narrow-band representation of ocean waves, 1. Theory, J. Geophys. Res. 91 (C6) (1986) 7743–7752.
[10] D. Middleton, An Introduction to Statistical Communication Theory, 3rd edition, IEEE Press, Piscataway, NJ, 1996.
[11] P.M. Woodward, The spectrum of random frequency modulation, Technical memorandum, Telecommunications Research Establishement, Great Malvern, Worcs., England, 1952.
[12] S.H. Crandall, Perturbation techniques for random vibration of nonlinear systems, J. Acc. Soc. America 35 (11) (1963) 1700–1705.
[13] N.M. Blachman, G.A. McAlpine, The spectrum of a high-index fm waveform: Woodward's theorem revisited, IEEE Trans. Comm. Tech. COM-17 (2) (1969) 201–207.
[14] Y.C. Kim, E.J. Powers, Digital bispectral analysis and its applications to nonlinear wave interactions, IEEE Trans. Plasma Sci. PS-7 (2) (1979) 120–131.
[15] M.K. Ochi, K. Ahn, Probability distribution applicable to non-Gaussian random processes, Prob. Engrg. Mech. 9 (1994) 255–264.
[16] M. Coantic, A. Favre, Activities in and preliminary results of air-sea interaction research at I.M.S.T, Adv. Geophys. 16 (1974) 391–405.
[17] A. Molinaro, Ya.D. Sergeyev, An efficient algorithm for the zero crossing detection in digitized measurement signal, Measurement 30 (2001) 187–196.
[18] P.M. Oliveira, V. Barroso, Definitions of instantaneous frequency under physical constraints, J. Franklin Inst. 337 (4) (2000) 303–316.
[19] T. Elfouhaily, D.R. Thompson, L. Linstrom, Delay-Doppler analysis of bistatically reflected signals from the ocean surface: theory and application, IEEE Trans. Geosci. and Remote Sens. 40 (3) (2002) 560–573.